Investigation into the Accuracy, Efficiency and Applicability of the Method of Moments as Numerical Dosimetry Tool for the Head and Hand of a Mobile Phone User

FJC Meyer*, KD Palmer! and U Jakobus+

* EM Software & Systems SA(EMSS), Stellenbosch, South Africa: E-mail: fjcmeyer@emss.co.za
! University of Stellenbosch, Stellenbosch, South Africa: E-mail: palmer@ing.sun.ac.za
+ Institut für Hochfrequenztechnik, Univ. Stuttgart, Germany: E-mail: u.jakobus@ieee.org

ABSTRACT. **In this paper the Method of Moments (MoM) as numerical SAR assessment tool is investigated. Models for generic mobile phones operational at 900MHz and 1800MHz were developed. Simulations were performed using these phone models to investigate the accuracy and efficiency with which the MoM can predict field values inside lossy, dielectric test phantoms. Results obtained are compared to Finite Difference Time Domain (FDTD) simulations and measurements. Numerical simulations using the MoM were further performed using the generic phones, a parametric hand model and the preliminary standarised IEEE head phantom. Peak-SAR results are extracted from the MoM solutions and compared for different phone and hand positions, as well as with FDTD results where applicable.**

1 Introduction

The numerical method usually adopted for mobile phone characterization and Specific Absorption Rate (SAR) predictions is the Finite Difference Time Domain (FDTD) technique[1, 2, 3], or one of its derivatives. The popularity of the technique arises from its simplicity and its suitability to the highly inhomogeneous environment inside the human body. This makes SAR predictions possible in different parts of the body, e.g., the brain or the eye. The FDTD technique has however several drawbacks with respect to dosimetry calculations. These include: 1) difficulties in modeling some practical cellular phone antennas accurately; 2) limitations in modeling complex geometries due to the rectangular grids/meshes commonly associated with the technique, 3) requirement to include a discretized free-space region in the problem space. All these problems have been addressed by individual researchers working on the FDTD formulation in one way or another. However, special formulations are needed to overcome these problems, and the applicability of these is usually limited. An added advantage using the FDTD is that the solution in the time domain generates wide frequency band data. In most mobile phone applications this is not required, and a frequency domain method might be just as efficient for these monochromatic solutions.

The Method of Moments (MoM) technique is not widely used in numerical dosimetry. The most important reason for this is the severe computational restriction associated with a MoM formulation when highly inhomogeneous objects need to be considered. A MoM surface equivalence principle formulation[4] can, however, be used efficiently in numerical dosimetry when homogeneous phantoms are considered. For an inhomogeneous model of the body or head the FDTD technique cannot easily be avoided. However, recent results have shown that peak average SAR (an important quantity in compliance testing of mobile phones) calculations and measurements may be made using homogeneous phantoms[5, 6], for which the FDTD is no longer the obvious numerical method of choice. Using actual measurement in fresh cadavers the authors of [7] showed good agreement when comparing SAR values from homogeneous phantoms and cadavers for the brain, eye and inner ear. Homogeneous tissue material is sufficient for mobile phone antenna characterization because the influence of the human tissue on the antenna is insensitive to the inhomogeneities but rather depends on averaged material parameters of the head and hand. The use of homogeneous phantoms is also driven by the move to standardization of the measurement environment to allow calibrated SAR assessment to be done at various laboratories.

One of the goals of numerical dosimetry relating to mobile phone / human phantom interaction is to predict with the highest possible degree of accuracy the specific absorption rate (SAR) inside a human head model, without actually performing measurements. This requires confidence in the techniques employed and in the validity and accuracy of the mobile phone and human head models. There are three main aspects that would affect the accuracy of the numerical predictions. These are:
1) The accuracy with which the numerical phone models represent the electromagnetic features (antenna characteristics, radiating characteristics, etc) of real mobile

phones. To address this the development of generic phone models, based on two distinct classes of mobile phones on the market today, will be considered in section 2.
2) The accuracy with which the numerical techniques can calculate the fields inside phantom material. Validation comparisons of field predictions inside tests phantoms between the MoM, FDTD and measurements will be presented in section 3.
3) The validity of using a homogeneous generic human phantom head representing a highly inhomogeneous real human head. This has been discussed briefly above and also in the literature [5, 6], and an investigation on this for the generic phones and human phantoms used in this paper can be found in [8].

The effect of the human hand on mobile phone performance and peak SAR values in the head can be considerable. This is due to the possible close proximity of the lossy hand to the radiating structures of the mobile phone. The proximity to the mobile phone of the human head would, of course, also influence the phone characteristics. The shape of the head and presence of the hand both influence the power absorption and peak-SAR in the head. In section 4 hand and head models for the MoM are introduced. These models were used for power absorption calculations and SAR predictions in the hand and head of a mobile phone user, with the results obtained presented in section 5. The efficiency of the MoM as numerical dosimetry tool is also discussed in some detail for test phantoms in section 3, and human phantoms in section 6.

2 Generic Phones

For accurate numerical SAR calculations, mobile phones and their antennas must be modeled accurately. This is not a trivial exercise due to the geometric and component complexity of the phones that influences their electromagnetic radiation. Researchers use mobile phone models ranging from over-simplified [9, 10] to relatively complex and realistic constructions [11, 12]. After studying x-ray pictures of a number of modern mobile phones, two generic mobile phones were designed. These generic phones are based on actual cellphones and can be described as semi-realistic. The two generic phones selected are based on commercial phones operating in the GSM900 and GSM1800 bands. Numerical modeling and verification measurements of these two generic phones will be considered in this section.

2.1 Generic phone with helix type antenna operating at 900MHz

Modern mobile phones may be viewed from an electromagnetic point of view as constructed of three main parts: 1) antenna; 2) printed circuit boards and their components; 3) batteries. The antenna used with a range of 900MHz phones is a classical broadside mode helix. The body of the phone is modeled as a conducting rectangular box, enclosing the metallic parts of the phone. This generic phone represents a variety of mobile phones on the market today (an internal metallic casing is driven against a helix antenna, for operation at 900MHz).

Modeling of a helix type antenna with the MoM is relatively straightforward. However, care has to be taken that the segment thickness and lengths used to represent the helix do not violate any numerical discretization criteria. The phone base is modeled with an enclosed metallic box (using triangular surface patches). A short wire connects the base to the helix antenna. The first segment representing this short wire is where the model is fed using a voltage gap. The helix is modeled with 51 wire segments which closely resembles the geometry of the physical helix on the generic phone. Convergence studies show that the *body* of the generic phone is not very sensitive to different discretization sizes, as long as the basic rule of $\lambda/8$ or smaller for triangle side lengths is not violated. The helix part of the phone model is however very sensitive to discretization both in terms of accuracy and resulting resonance. This is in part due to the sensitivity of resonance to the length of the helix, where modifications to the discretization of the helix wire result in a change in the effective length of the helix and thus a change in resonant frequency. A segment discretization length of $\lambda/150$ or smaller on the helix antenna is required to ensure accurate and repeatable results.

The final MoM model is shown in figure 1. This relatively simple geometry provides a reasonable electromagnetic representation of a real phone with a helix type antenna. A physical model of the generic phone has been manufactured. On the physical model, the power is fed from the outside using a coaxial cable. Great care must be taken when doing this to prevent the generation of common mode currents on the feed cable — which has a considerable distorting effect on both radiation pattern and near-fields. The severity of this can be seen in figure 2. By calculating the near-fields around the phone (using numerical simulations), a region where the electric fields tangential to the feed are approximately zero was found near the center at the back of the phone. The insertion of the feed cable at this position has very little influence as no currents are generated on the cable. This was confirmed by comparing simulated and measured results — figure 3. Other tests performed, but not detailed here, also showed that the presence of the feed cable at the selected position had negligible effect on the fields inside phantoms with the phantoms in close proximity to the

generic phone.

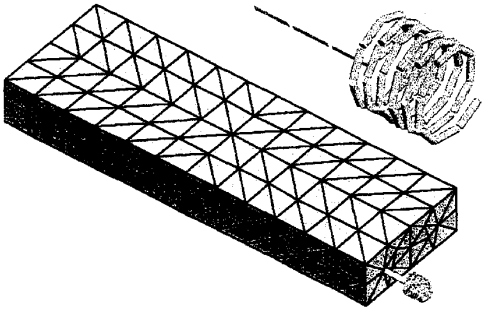

Figure 1: MoM model of Generic Phone 1 operational at 900MHz.

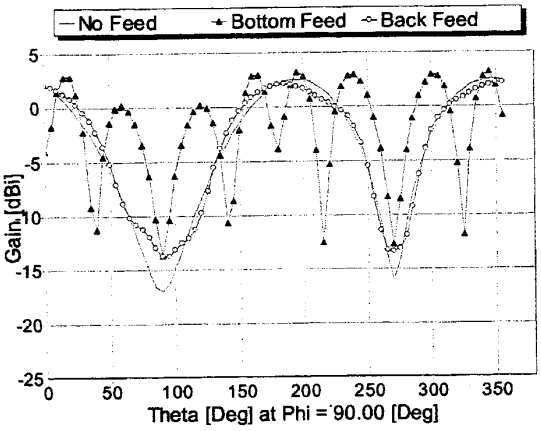

Figure 2: E-plane radiation pattern cut for Generic Phone 1 at 900MHz with and without feedwires. Results obtained with numerical simulations.

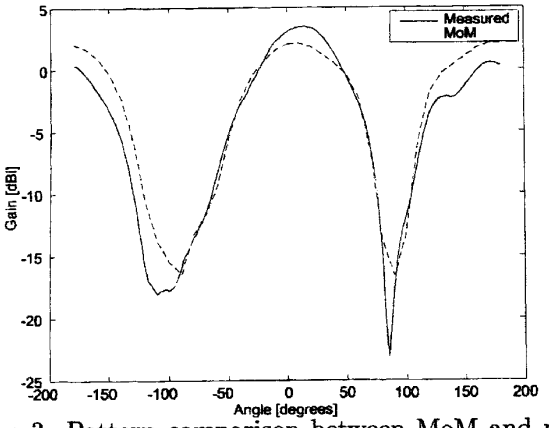

Figure 3: Pattern comparison between MoM and measurements for Generic Phone 1 at 900MHz.

2.2 Generic phone with inverted-F type antenna oprating at 1800MHz

A second slightly more complex phone model was used to investigate the operation of the newer generation of mobile phones. With respect to the radiation and dosimetry properties the two aspects of these phones that are important are the use of the 1800MHz frequency band and the switch to "internal" antennas. A study of the literature showed that the Planar Inverted-F Antenna (PIFA) is the most popular for internal operation. For this 1800MHz generic phone with a PIFA antenna, no detailed attempt has been made to model the body of the phone accurately. This is done for simplicity as the parts not included, e.g. battery box, printed circuit boards etc differ widely between phones. The generic design consists of a single flat plate representing the body of the phone, with the PIFA antenna mounted on the "top" of the side held away from the head. As was the argument against including the battery box and other details, for simplicity only a basic PIFA structure is used.

The generic phone at 1800MHz was derived by starting with a metallic plate the size of a typical modern 1800MHz phone, and then designing a PIFA to mount on the outside top. This deceptively simple geometry is a reasonable representation of a real phone from an electromagnetic point of view, and a physical model has been built to allow comparison of measured and simulated results. The MoM model and physical phone are shown in figures 4 and 5 .

Due to its design, this generic phone model is very sensitive to small displacements in feed pin and shorting plate position and size. For this reason the MoM model might also be sensitive to the discretization of the model. A convergence study was performed to investigate the MoM discretization criteria required to have confidence in the model. Results indicate some shift in frequency due to the different discretizations. A discretization criteria of $\lambda_0/40$ or smaller is acceptable and was used for all subsequent MoM simulations involving this generic phone.

Similar to the 900MHz generic phone, the physical phone model at 1800MHz is fed externally using a coaxial cable, and positioning of this cable on the phone was critical to avoid common mode currents on the feed cable. An optimal position was found at the back of the phone (see figure 5).

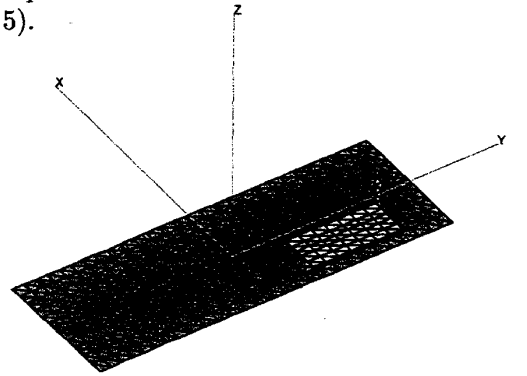

Figure 4: MoM model of Generic Phone 2 operational at 1800MHz.

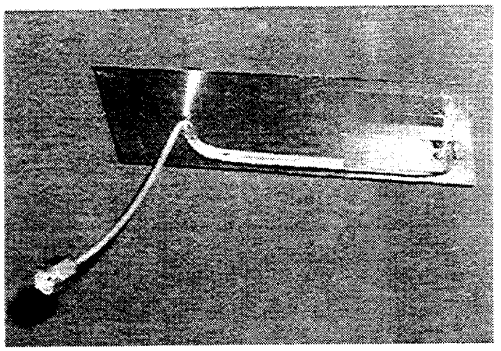

Figure 5: Physical model of the generic phone for operation at 1800MHz.

2.3 S11 calculations for generic phones

The numerical MoM code FEKO [13] was used to model the generic phones described in the preceding sections. Before detailed SAR calculations were made, an initial verification of the model and numerical technique was carried out. The first validation selected was that of input impedance and the derived reflection coefficient (or S_{11}) because this is one of the most sensitive parameters by which to gauge the accuracy of a numerical solution. S_{11} results can be used to assess how well the numerical solution is able to model the power reflected by the antenna. The physical model input impedance was measured in an anechoic chamber. Input impedance results between MoM and measurements shown in figures 6 and 7 compare very well at 900MHz and reasonably well at 1800MHz. This indicates that the numerical models are able to predict the resonant frequency and reflected power very well.

3 Field Calculations inside Test Phantoms

The Specific Absorption Rate, or SAR, with units W/kg can be calculated as:

$$SAR = \frac{1}{2}\sigma\frac{|E|^2}{\rho} \qquad (1)$$

with σ the conductivity (S/m),and ρ the mass density (kg/m^3) of the tissue material. For homogeneous phantoms, both σ and ρ are constant. To investigate the accuracy and efficiency with which the MoM can be used for SAR predictions inside a lossy phantom, field values ($|E|^2$) inside test phantoms were compared for numerical simulations and measurements. Measurements were performed in the EMSS dosimetry lab. The main "features" of the lab are described in [14] with details in [15]. In particular, the probe used for the measurements was purchased from Schmid & Partner Engineering [16]. Measurement and simulations are presented for 1W (time averaged) input power, and no normalization

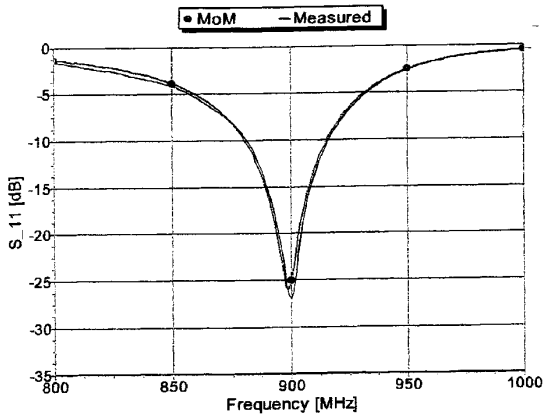

Figure 6: Reflection coefficient comparisons between MoM model and measurements for Generic Phone 1 operational at 900MHz.

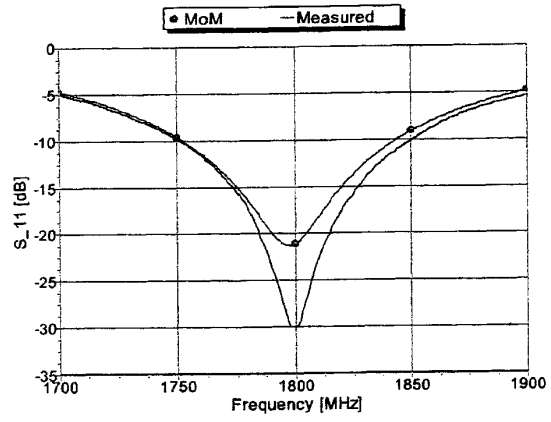

Figure 7: Reflection coefficient comparisons between MoM model and measurements for Generic Phone 2 operational at 1800MHz.

was performed to improve the absolute agreement between results.

Test antennas (dipoles) and the generic phones of the previous section were used together with a box and a sphere phantom, at both 900MHz and 1800MHz. Results for the box phantom will be presented here. The physical rectangular box phantom consists of a 1mm fibre-glass outer casing. The box is filled with equivalent brain tissue material to a height of 75mm. The material parameters of the brain tissue equivalent are $\epsilon_r = 42.33$, $\sigma = 0.855$ [S/m] at 900MHz and $\epsilon_r = 34.83$, $\sigma = 1.726$ [S/m] at 1800MHz (material and material parameters provided by Schmid & Partner Engineering [16]). When filled with phantom material the box phantom bulges downwards by 3mm due to the weight of the tissue material. This distorts the shape of the "rectangular" phantom, but the distortion is less than 1mm over the length of any of the antennas under tests. None of the numerical models include the fibre-glass casing, and only the antennas and the phantom material are modeled.

Comparison between measurements and numerical simulations for the *dipole antennas* and test phantoms agree well. The only discrepancies are for values below the noise floor of the measurements system. This is at about 15dB-V/m corresponds to about 0.013W/kg in brain tissue equivalent at 900MHz (well below the ICNIRP[17] basic restriction of 2W/kg). These results are not presented here and can be found in reference [8]. Field results for the *generic phones* and test phantoms will be presented in subsequent sections, but the MoM discretization requirements for the lossy dielectric box phantom will first be discussed.

3.1 Discretization Criteria

The MoM has the general discretization rule that the triangle patch edge length should be less than about $1/6^{th}$ of a wavelength. For the surface equivalence principle used with dielectric bodies, this criterion must be applied to the wavelength in the dielectric medium. For the dipole or generic phone / box phantom simulations this means that the discretization requirements on the dielectric phantom dominate the computer requirements. Numerical tests showed that the discretization requirements can be relaxed without losing much accuracy in terms of field calculations close to the source. This is shown in figure 8 where the field values along a line inside the phantom are compared for various MoM solutions with different discretizations. The memory requirements and solution times for the different surface discretizations are given in table 1. A variable discretization[1] with a $\lambda_r/6{:}3{:}1.5$ distribution is less than 0.2dB off from the reference solution which is well within the accuracy required. This is at peak field values, 1mm from the phantom side. The advantages of using a discretization of $\lambda_r/6{:}3{:}1.5$ are clear from the computer requirements listed in table 1.

At 1800MHz the advantage of this variable discretization is more profound due to the increase in computer requirements. Memory requirements and solution times for the different surface discretizations are also given in table 1. Here again a $\lambda_r/6{:}3{:}1.5$ discretization results in peak field values less than 0.25dB off from the reference solution.

The MoM model with variable discretization is shown in figure 9. From the results presented here and other results obtained it is clear that the variable discretization of $\lambda_r/6{:}3{:}1.5$ on the phantom can be used, provided that $\lambda_r/6$ discretization is used on the surface region close to the source antenna. The reason for this is that a fine discretization in this region results in accurate representation of the equivalent currents. It is the equivalent surface current in this region (close to the source) that have the most significant effect on the peak field values in the dielectric. (The field values inside the dielectric are calculated by integrating the equivalent surface currents over the whole dielectric surface.) A course discretization on the dielectric surface *far* from the source antenna results in an average, but not highly accurate, equivalent surface current representation. These currents contribute much less to the peak field values in the dielectric.

[1]Variable discretization of $\lambda_r/$A:B:C means that $\lambda_r/$A is used in one part of the model (usually close to the source), $\lambda_r/$B in a second part and $\lambda_r/$C in the third, least significant, part of the model.

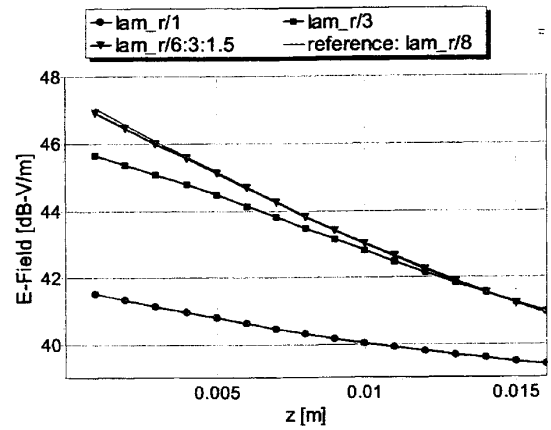

Figure 8: Electric field values calculated along a z-line inside the box phantoms with various discretizations used on the surface of the phantom.

Discretization	Sol. Time [sec]	Memory [MB]
900 MHz		
$\lambda_r/1$	31	2.3
$\lambda_r/3$	248	39.5
$\lambda_r/5$	1210	237.2
$\lambda_r/6{:}3{:}1.5$	183	25.7
1800 MHz		
$\lambda_r/1$	40	5.6
$\lambda_r/2.9$	985	233.1
$\lambda_r/5$	9644	1921.7
$\lambda_r/6{:}3{:}1.5$	651	159.5

Table 1: Solution times and memory requirements for MoM solutions with various discretizations on the box phantom. See footnote 1 for definition of variable discretization $\lambda_r/$A:B:C. Results obtained on a 4-PC 350MHz Pentium II Parallel Linux Cluster.

3.2 Field Comparisons for Generic Phones and Test Phantoms

The generic phones at 900MHz and 1800MHz were next used for field measurements and simulations inside the test phantoms. Variable discretizations (as discussed in the previous section) were used on the test phantoms and generic phones, with a fine discretization on the surface of the phantom adjacent to the generic phone structures.

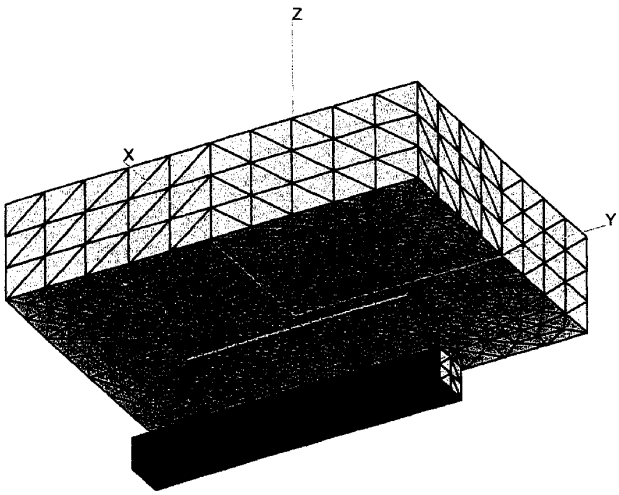

Figure 9: MoM models of the 900MHz dipole and box phantom with variable discretization.

Field results along a line (y-line) are shown in figures 10 and 11. At 900MHz the MoM predictions have an offset of about 1.3dB at peak field values in the phantom when compared to measurements. This might be due to some remaining uncertainties concerning the actual power radiated by the physical generic phone when close to the phantom material. The MoM results are also compared to FDTD results (obtained with the FDTD code Totem [18]) for the same phone and phantom. The agreement is good, but notice the difference in shapes on the y-line at about 0.06m. The MoM and measurement shapes are in good agreement but the FDTD has a different structure. This is due to the simplified modeling of the helix antenna with the FDTD technique (see reference [19]). It is important to note that this simplified modeling of the helix antenna is a limitation of the FDTD used in this study, and not a general limitation of the FDTD technique, as was shown in recent findings [20].

At 1800MHz the peak field values of the measured, MoM and FDTD results agree well but the shape or structure along the y-line differs (figure 11). This is certainly above the measurement system noise floor. Field distributions along the x- and z-lines for these phones and phantom (not presented here) show a similar tendencies, with good agreement between MoM, FDTD and measurements at 900MHz and reasonable but not very accurate agreement at 1800MHz. An investigation into this matter revealed that the positioning of the generic phone, when performing measurements, was not assessed accurately enough. The field distribution inside the phantom seems to be highly sensitive to the distance between phone and phantom. This is more so than with the 900MHz generic phone, and mainly because the phantom is on the "back-lobe-side" of this 1800MHz generic phone (see reference [19]). This "back-lobe-side" is also the reason for lower field values inside the phantom when compared to the generic phone at 900MHz. The argument that a higher degree of accuracy is needed in phone positioning, to improve comparisons with numerical results, still needs to be confirmed. Another possibility that could be investigated is the effect that the 1mm fibre-glass casing of the phantom has. This was not included in any of the numerical models.

3.3 Generic Phones vs Real Mobile Phones in Test Phantoms

The 900MHz and 1800MHz generic phones are based on two commercially available mobile phones. To investigate how closely these generic phones represent real phones, field measurements inside the box phantom (filled with equivalent brain tissue material) were performed with both phones in close proximity to the phantom. Measurements along a number of line cuts inside the phantom were performed. The results for a y-line cut at 900MHz and 1800MHz are shown in figures 10 and 11. Again, field values are presented for 1W, time averaged, input power. (Normalized to 1W in the case of the real mobile phones operating at full power of: 250mW and 125mW, time averaged, at 900MHz and 1800MHz respectively.)

The results show good agreement for the 900MHz phone and reasonable agreement for the 1800MHz phone. Bear in mind that the real mobile phones are vastly more complex in geometric structure than the generic phones. It is clear that the generic phones embody the main radiating components of the real phones they were based on.

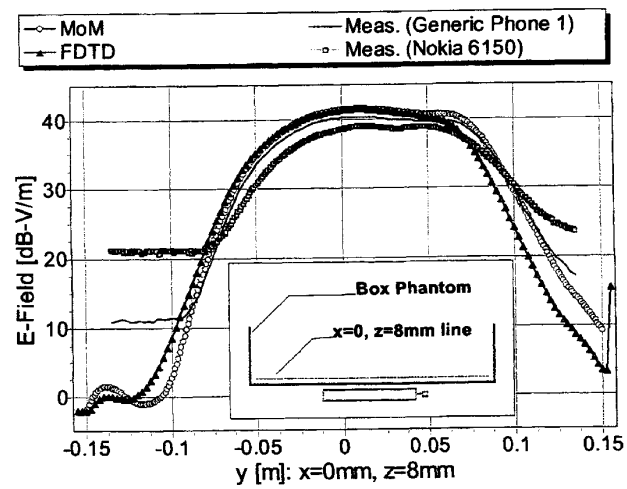

Figure 10: Electric field predictions and measurements inside the box phantom. Source: Generic phone at **900MHz**. Distance between phone top and phantom material: 6mm.

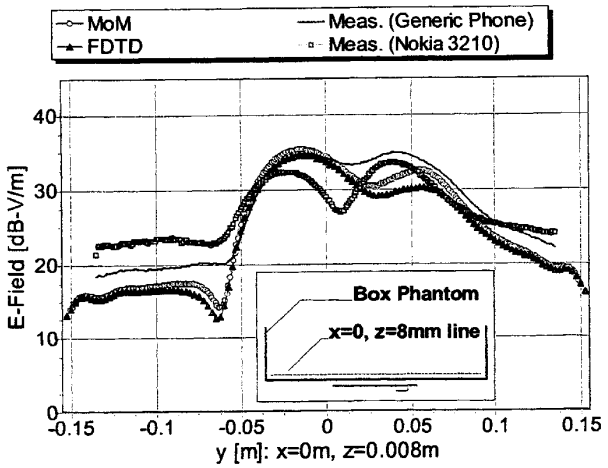

Figure 11: Electric field predictions and measurements inside the box phantom. Source: Generic phone at **1800MHz**. Distance between phone top and phantom material: 6mm.

4 Human Models

4.1 Modeling of the Hand

The inhomogeneous nature of the hand can easily be handled by the FDTD technique, but the exact positioning of the hand in a realistic position around the mobile phone is not very easy (although the use of a fully-articulated realistic hand within the FDTD algorithm has recently been reported [21]). As could be expected, and also shown by researchers[9, 10], the hand does have an effect on energy absorption and maximum SAR in the head of the user. The energy absorption in the hand is significant because it is close to the mobile phone antenna. It also changes the radiation pattern of the phone.

For the MoM simulations a *parametric* hand model can be used. The hand model must be homogeneous to apply the MoM surface equivalence principle. A current limitation of the MoM as implemented in FEKO[13] is that only one dielectric material can be used for one or more closed dielectric objects in the MoM problem space. For this reason, the material parameters used for the homogeneous MoM model are that of equivalent brain tissue (as supplied by SPEAG [16] at 900MHz and 1800MHz). Numerical studies performed using the FDTD technique and dipole antenna[8] show that this homogeneous hand should over-predict the energy absorption in the hand by about 10% at 900MHz and under-predict the absorption at 1800MHz by about 10%. Note that the exact percentage of error will be source type and source position dependent. But 10% does, however, give a quantitative indication of the error introduced when using a homogeneous hand model. The obvious drawback of the MoM is that the hand model must be homogeneous, but this is weighed against the accuracy with which the hand geometry and positioning can be modeled.

The parametric hand model has more than 20 degrees of freedom associated with it (defined in terms of parametric variables in the model file). By changing one or more of these variables, the hand model can be rotated, translated and /or reshaped in the MoM problem space. The hand can thus, with ease, be positioned in almost any position around the phone. One such position around the 900MHz generic phone is shown in figure 12.

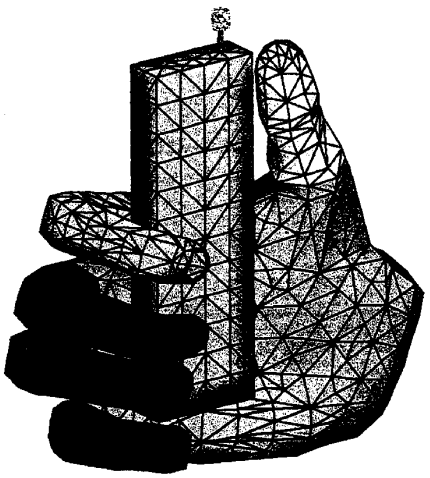

Figure 12: Homogeneous MoM hand with generic phone operating at 900MHz.

4.2 Modeling of the Head

The human head, and indeed the whole human body, is a highly inhomogeneous object with different tissue materials having wide ranging electromagnetic parameters. These parameters are also frequency dependent. The parameters of interest in SAR assessment are the permitivity (ϵ_r), conductivity (σ [S/m]) and mass density (ρ [kg/m^3]) of the tissue material.

The shape of the human head also has an affect on the SAR distribution. A generic human head (representative of the mobile phone user population) is under development by the IEEE [22]. The aim is to standardize the head that will be used for SAR compliance testing of cellphones. The shape of the phantom head for these measurements is also being standardized and a preliminary shape has been obtained from SPEAG [16]. No information could be obtained regarding the dimensions (size in particular, the shape is fixed) of this phantom. It was decided to scale the preliminary IEEE head phantom to the head size given in reference [23] which, in turn, refers to reference [24]. Although this will not be exactly the size of the final IEEE SCC34 generic head phantom, it should be very close. It must also be mentioned that the preliminary IEEE head phantom has been numeri-

cally decapitated (i.e., the shoulders were removed at the level of the neck).

The MoM model is a very accurate representation of the phantom geometry. This is made possible because triangular patches are used with the MoM to represent the outside surface area of the phantom. The FDTD model used has a 2.5mm resolution regular grid model, and regions around the ear are not represented very accurately with this model. A finer grid (at least in the area of the ear, close to the mobile phone) is required to improve on this situation.

The MoM model of the IEEE generic head is shown in figure 13. The FDTD model of the same head used for comparison with MoM results are also shown this figure.

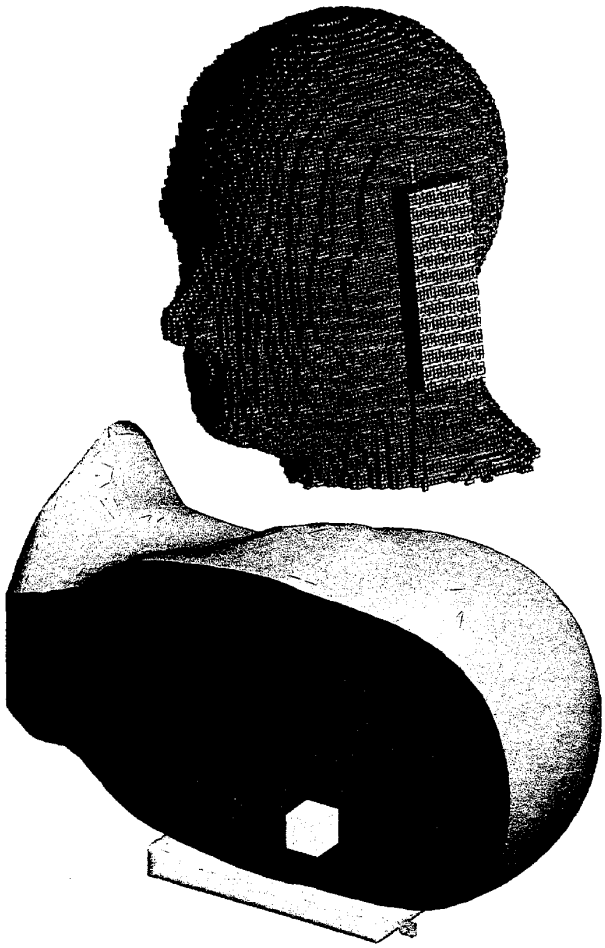

Figure 13: IEEE generic head models used for SAR assessment with the generic phone at 900MHz. FDTD model (top) and MoM model (bottom). The peak-SAR-Cube$_{10g}$ volume for the MoM solution is also shown.

5 Power Absorption and SAR Results

In the introduction three main aspects that would determine the accuracy with which numerical techniques can predict SAR in a human phantom were discussed. To recap, 1) the ability of the techniques to model mobile phones, 2) the accuracy of field predictions in equivalent phantom tissue, 3) the validity of phantom models as replacements for human operators (and in particular for this study, the human head). The first two aspects were considered in preceding sections of this paper and the third was investigated in references [8].

It has been established that the MoM can model generic phones accurately and these generic phones are reasonable representations of actual phones (within 2-3dBs as indicated by measurements). The numerical field calculations in homogeneous phantoms are accurate within one or two dBs when compared to measurements. The use of homogeneous phantoms (head and hand) results in energy absorption (or SAR) calculations within 10%-20% accuracy when compared to inhomogeneous phantoms. With this knowledge, numerical SAR assessment was performed using the generic phone models, the preliminary IEEE phantom head of section 4.2 and the parametric hand presented in section 4.1. The results obtained will be discussed in this section.

5.1 Power absorption in the hand

The MoM hand model introduced in section 4.1 was used with the generic phones to investigate the energy absorption in the hand, and the effect of the hand on the radiation pattern and input impedance of the phone. The models used are shown in figure 12. The hand model was maneuvered to positions around the phone representing a typical position in which a user might hold a mobile phone.

The power absorption in the hand (without the presence of the head) is summarized in table 2. At both frequencies the percentage absorption is surprisingly high. At 900MHz the effect of the hand on the radiation pattern is relatively small, but the effective gain is of course reduced considerably due to the high percentage of energy absorption. More significant is the effect of the hand on the 1800MHz generic phone. Two typical positions were investigated. In the one scenario, the hand is held clear from the inverted-F patch and in the second scenario the hand partially covers the patch. From the results in table 2, and other results obtained but not presented here, it is evident that for the 1800MHz generic phone, the precise hand position is critical in terms of power absorption. Covering of the patch means more energy into the hand and less radiated away.

5.2 Peak SAR extraction

ICNIRP[17] requires that the peak SAR, as averaged over any 10g of contiguous tissue, be used for compliance testing of mobile phones. The old ICNIRP standards required peak SAR calculations in 10g tissue material in

Hand Position	Absorption Ratio [%]
900 MHz:	
Clear from helix	61.2
1800 MHz:	
Clear from patch	41.9
Partially covers patch	72.6

Table 2: Power absorption in the MoM hand model with generic phones at 900MHz and 1800MHz. This is as a percentage of total input power.

the shape of a cube. The IEEE standards[25] require peak SAR calculations in 1g tissue material in the shape of a cube. The basic restriction for localized exposure in the head of a user, as determined by ICNIRP is 2W/kg. The IEEE uses 1.6W/kg as basic restriction.

In this paper both *peak SAR averaged over any 10g of contiguous tissue* and *peak SAR calculations in 10g tissue material in the shape of a cube* were used. These will be denoted by peak-SAR-Contigeous$_{10g}$ and peak-SAR-Cube$_{10g}$ respectively. For the MoM implementation in the program FEKO[13], post-processing algorithms for the extraction of peak-SAR-Cube$_{10g}$ and peak-SAR-Contigeous$_{10g}$ were developed. Results obtained with these will be presented below, and the algorithms are discussed in detail reference [8].

Figure 14: MoM model of IEEE generic head, hand and generic phone at 1800MHz. Peak-SAR-Contigeous$_{10g}$ volume is also shown.

5.3 SAR results in the IEEE phantom head

Using the SAR extraction routines discussed in the previous sections, SAR results were obtained for the generic phones and IEEE phantom. This was done using the MoM as well as the FDTD technique. With the FDTD, the alignment of the generic phones are next to the ear of the phantom, parallel to the vertical axis (see figure 13 - top). For comparison, a similar alignment of the phones for the MoM was adopted (figure 13 - bottom). Simulations with the MoM (only) were also performed with the phones in a more representative talking position — next to the ear, rotated in such a way that the bottom of the phones points towards the mouth of the phantoms (see figure 14). In these simulations the MoM hand model was also included. The results obtained are summarized in table 3.

The results show very good agreement in peak-SAR and total head absorption obtained with the FDTD and MoM solutions. Total absorption and peak-SAR are lower with the 1800MHz generic phone. The presence of the hand increases the total absorption (head and hand) but decreases the peak-SAR for the 900MHz phone. For the 1800MHz phone, the movement of the phone into a realistic talking position increases the peak-SAR significantly (by a factor of about three). This emphasizes the point that peak-SAR is highly dependent on phone positioning. The presence of the hand in this 1800MHz case, increases absorption by a factor of two, and the peak-SAR in the head is **increased**. This means that exclusion of the hand in peak-SAR calculations, results in an under-estimate of SAR — for this phone in this specific position (an important result that must be investigated further).

Another important observation is that the peak-SAR-Contigeous$_{10g}$ in the head is between 10% and 40% higher than the corresponding peak-SAR-Cube$_{10g}$ (depending

Numerical Model	Head absorption [W]	peak-SAR Cube$_{10g}$ [W/kg]	peak-SAR-Contig$_{10g}$ [W/kg]
900-MHz:			
FDTD-GP1-M1	0.69	4.16	—
MoM-GP1-M1	0.74	4.27	5.63
MoM-GP1-M2	0.94	3.91	4.29
1800-MHz:			
FDTD-GP2-M1	0.21	1.2	—
MoM-GP2-M1	0.31	1.37	1.91
MoM-GP2-M2	0.68	4.06	5.36
MoM-GP2-M3	0.33	3.78	4.80
MoM-GP2-M4	0.31	3.62	4.67

M1: Phone next to ear aligned parallel to the vertical axis of the head — see figure 13

M2: Hand included and phone next to ear with base of phone running along the cheek to the mouth of the phantom — see figure 14.

M3: Same phone position as M2 but without the hand.

M4: Same as M3 but with variable discretization on head phantom to reduce computer requirements — see table 4 for details.

Table 3: SAR results for generic phone at 900MHz and 1800MHz with IEEE phantom. All values normalized to 1W (time averaged) input power. For MoM-GP1-M2 and MoM-GP2-M2 hand absorption is included.

on phone position). Keep in mind that peak-SAR-Contigeous$_{10g}$ is what the latest ICNIRP standards require. The peak-SAR-Cube$_{10g}$ and peak-SAR-Contigeous$_{10g}$ positions inside the phantoms are shown in figures 13 and 14.

6 Numerical considerations for generic phones and IEEE phantom models

In the previous section, the SAR results for the generic phones and IEEE phantom were presented. Both FDTD and MoM techniques require a considerable amount of hardware resources for these problems because of the complexity of the models. Also, by nature of the models, only geometric symmetry for the phantom head (about one plane) could be exploited. The model information and computer requirements are summarized in table 4. The times are normalized for a 4-PC 350MHz Pentium II Parallel Linux Cluster (except where explicitly mentioned otherwise).

For the 900MHz problems, the MoM compare favorably to the FDTD solution with respect to solution times. At 1800MHz the MoM solution time is an order of magnitude more than that of the FDTD solution. However, the FDTD model is a 2.5mm resolution model and a finer resolution model is needed for more accurate geometric modeling of the head phantom (as discussed in section 4.2). The implication here is that the FDTD solution time and memory requirements would increase considerably. Also, if a MoM model with variable discretization is used (model number MoM-GP2-M4) then the difference in MoM and FDTD solution time requirements are decreased significantly. A comparison of the power absorption results (see table 3) for MoM-GP2-M3 (fine discretization all over on head) and MoM-GP2-M4 (variable discretization on head) shows that there is less than 3% difference in peak-SAR values for these two models and the computer requirements for MoM-GP2-M4 is much lower than for MoM-GP2-M3. This confirms again the observation made in section 3.1 that MoM models with variable discretizations on the dielectric regions can be used for SAR calculations as long as a sufficiently fine discretization is used close to the source antenna.

At both 900MHz and 1800MHz the MoM memory requirements are considerably more than that of the FDTD, but a fast parallel block LU decomposition implementation reduces this to harddisk memory availability only (see **Memory for MoM** description at the bottom of table 4). All data for the MoM is based on a traditional implementation. A significant reduction of both memory and CPU-time can be expected when using accelerations such as FMM or AIM [26].

7 Conclusions

This paper presents the development of generic phone models representing a wide class of real mobile phones operating at 900MHz and 1800MHz. Generic phones have the advantage of being complex enough to realistically represent real phones (as confirmed by measurements), but simple enough that one can extract controlled and detailed information on the capabilities and short-comings of numerical techniques to model mobile phones and their antennas. Two generic phones were designed and manufactured resulting in physical phones that could be used in laboratory experiments. The investigation revealed the importance of giving attention to the possible influence that the feed cable of generic phones might have. The accuracy and efficiency of the numerical models of the phones were investigated and compared to measurements where appropriate. The generic phones developed encompass the main antenna characteristics of real mobile phones. This is confirmed by measurements, where field values produced by generic and commercial (real) mobile phones inside a box phantom were compared.

Four test antennas (two dipoles and two generic phones) and two test phantoms were used for validation tests involving interaction between antennas and simulated human tissue at 900MHz and 1800MHz. The most important modeling requirements were considered which included discretization criteria, solution times and memory resources. With the MoM surface equivalence principle implementation, variable discretization can be used on the phantom surface without compromising the geometric accuracy of the problems. This reduces the resource requirements of the MOM considerably and brings it on par with the FDTD — at least for single frequency solutions. Results obtained show, in general, excellent agreement between electric field values inside the phantoms computed using the MoM and FDTD techniques. Field results from both techniques agreed, in most cases, very well with measurements. Discrepancies of note observed are when field values are lower than the noise floor for the measurement system. Also, for the generic phone at 1800MHz, the structure of the field distributions just inside the phantom differed between measurements and computations, possibly due to the sensitivity of exact phone positioning for this generic phone at 1800MHz.

A parametric MoM hand model was introduced. This hand model is very flexible in terms of positioning but due to the formulation the model represents a homogeneous hand. Absorption in the hand when holding the generic phones was calculated. Results showed that between 40% and 70% of the power is absorbed by the hand, dependent on its exact position.

For standardized SAR calculations generic homogeneous phantom head models, as proposed by the IEEE, were developed for use with both the MoM and FDTD techniques. Peak SAR extraction routines both for 10g of tissue in the shape of a cube, and also for 10g contiguous tissue were considered. The SAR results obtained showed very good agreement between FDTD and MoM results (where applicable). The effect of the hand on peak-SAR in the head is relatively small, reducing it by about 10% at 900MHz, but increasing it by a few percent for the 1800MHz phones. This result at 1800MHz must be repeated for more hand/phone positions to establish if it is true in general. For both generic phones and for the different scenarios investigated, the peak-SAR-Contigeous$_{10g}$ (as required by ICNIRP[17]) is more (up to 40% in some cases) than the peak-SAR-Cube$_{10g}$ which is used most often in SAR compliance tests.

Numerical consideration for generic phones / IEEE phantom models of the FDTD and MoM techniques was discussed. With both techniques these models can be solved on averaged PC-clusters and workstations, within hours. The memory requirements are considerable, especially with the MoM models, but an efficient out-of-core solver reduces this requirement to available disk space. The FDTD technique is certainly the most efficient, especially if wide-band information is required, but the MoM has several important advantages related to accurate geometric modeling. Apart from the numerical differences, the two techniques also differ in the way that the biological tissue is represented in the problem space. With the MoM biological regions are of course represented by equivalent currents flowing on the surface. With the FDTD, biological regions are represented directly by the fields induced in the penetrable tissue material. With the MoM equivalent surface solution, coupling between head, hand and antenna can thus be interpreted as source / induced current interactions. This allows for additional physical insight into the problem when considering antenna performance, when in close proximity to human phantoms.

From the results obtained, we are confident that the peak average SAR predictions presented in this report are accurate to within a few dBs. This is unfortunately not yet accurate enough to replace measurements as compliance evaluator, but it is certainly accurate enough for investigating the expected peak average SAR values from different mobile phone antenna types. A number of aspects could be addressed to improve the accuracy of the numerical results. It is, for example, believed that better agreement between measurements and simulations is possible if more attention is given to accurate positioning of the phones when measurements are performed. The influence of hand / head position next to the phone on peak-SAR could also be investigated further in an effort to quantify the range of local exposure that could be expected. However, the main room for improvement in

Model Number	Model Size	discretization	Memory [MBytes]	Solution Time [Hours:Min]
900MHz				
FDTD-GP1-M1	380 x 400 x 260:2.5	20.4	400	1:35
MoM-GP1-M1	2338:1152:54	32.0	1455.2:128	1:13
MoM-GP1-M2	4122:336:54	43.7	2881.0:128	2:32
1800MHz				
FDTD-GP2-M1	380 x 400 x 260:2.5	11.4	420	1:36
MoM-GP2-M1	8378:1048:3	37.9	11944.0:180	24:24
MoM-GP2-M2	11866:748:3	39.6	20592.2:192	70:16
MoM-GP2-M3	8378:748:3	37.9	11905.0:180	29:32
MoM-GP2-M4	4916:748:3	72/36/18	4050.5:128	4:15

Model Number:	See caption of table 3 for model number description.
Model Size for FDTD:	X x Y x Z dimensions in mm: Cell size in mm.
Model Size for MoM:	Dielectric-Triangles: Metallic-Triangles: Metallic-Segments.
discretization for FDTD:	Cells per wavelength in dielectric.
discretization for MoM:	Average number of dielectric triangles per square wavelength in dielectric. For MoM-GP2-M4, with variable discretization, A/B/C represents the fine, medium and coarsely discretized regions on the head model.
Memory for FDTD:	Total memory requirements related to both nodes on a duel-processor SGI workstation.
Memory for MoM:	A:B, with A $->$ Total memory requirements : B $->$ Memory blocks used on 4-node Linux Cluster. In practice this means that B MBytes of RAM are needed per Linux Cluster node and that A MBytes of free disk space is required.
Solution Time for FDTD:	Obtained on a duel-processor SGI workstation, and normalized to a 4-PC 350MHz Pentium II Parallel Linux Cluster.
Solution Time for MoM:	Obtained on a 4-PC 350MHz Pentium II Parallel Linux Cluster. MoM-GP2-M1, MoM-GP2-M2 and MoM-GP2-M3 were solved on a heterogeneous 5 node PC Linux Clusters. The solution times for these models **were** normalized to that of the 4-node PC cluster.

Table 4: Model information and computer requirements for generic phones with IEEE phantom.

accuracy is the development of even more realistic generic phone models.

References

[1] A. Taflove, *Advances in Computational Electrodynamics: The Finite Difference Time Domain Method.* Artech House, 1998.

[2] G. Lazzi, S. S. Pattnaik, and O. P. Gandhi, "Experimental and FDTD-computed radiation patterns of cellular telephones held in slanted operational conditions," *IEEE Trans. Electromag. Compat.*, vol. 41, pp. 141–144, May. 1999.

[3] C. M. Furse and O. P. Gandhi, "A memory efficient method of calculating specific absorption rate in CW FDTD simulations," *IEEE Trans. Biomed. Eng.*, vol. 43, pp. 558–560, May 1996.

[4] U. Jakobus, "Comparison of different techniques for the treatment of lossy dielectric/magnetic bodies within the method of moments formulation," *AEÜ International Journal of Electronics and Communications*, vol. 54, no. 3, pp. 163–173, 2000.

[5] K. Meier, V. Hombach, R. Kastle, R. Y. Tay, and N. Kuster, "The dependence of electromagnetic energy absorption upon human-head modeling at 1800 MHz," *IEEE Trans. Microwave Theory Tech.*, vol. 45, pp. 2058–2062, Nov. 1997.

[6] V. Hombach, K. Meier, M. Burkhardt, E. Kuhn, and N. Kuster, "The dependence of EM energy absorption upon human head modeling at 900 MHz," *IEEE Trans. Microwave Theory Tech.*, vol. 44, pp. 1865–1873, Oct. 1996.

[7] G. Neubauer, G. Schmidt, H. Molla-Djafari, and F. Alesch, "SAR Evaluation in Human Heads," in *Paper presented at BEMS'99*, (Long Beach, CA, USA), 1999.

[8] F. J. C. Meyer and K. Palmer, "Numerical dosimetry research at EMSS: Energy absorption in the head and hand of a cellphone operator.," Tech. Rep. 2000_P02_52a, EM Software & Systems, Quantum Building, Technopark, Stellenbosch, South Africa, www.emss.co.za, July 2000.

[9] M. Okoniewski and M. Stuchly, "A study of the handset antenna and human body interaction," *IEEE Trans. Microwave Theory Tech.*, vol. 44, pp. 1855–1864, Oct. 1996.

[10] S. Watanabe, M. Taki, T. Nojima, and O. Fujiwara, "Characteristics of the SAR Distributions in a Head Exposed to Electromagnetic Fields Radiated by a Hand-Held Portable Radio," *IEEE Trans. Antennas Propagat.*, vol. 44, pp. 1874–1883, Oct. 1996.

[11] M. Rahman, M. Stuchly, and M. Okoniewski, "Dual-band strip-sleeve monopole for handheld telephones," *Microwave and Optical Technology Letters*, vol. 21, pp. 79–82, Apr. 1999.

[12] P. Bernardi, M. Cavagnaro, and S. Pisa, "Evaluation of the SAR distribution in the human head for cellular phones used in a partially closed environment," *IEEE Trans. Electromag. Compat.*, vol. 38, pp. 357–366, Aug. 1996.

[13] FEKO Suite 2.5, *www.feko.co.za.* EM Software & Systems, South Africa, April 2000.

[14] L. J. du Toit and F. J. C. Meyer, "Functionality Validation and Error Estimation Procedures Pertinent to the Upgrading of a Hybrid RF Dosage Assessment System," in *Proceedings of the 22nd Bioelectromagnetics Society Meeting*, (Munich, Germany), p. 231, Jun. 2000.

[15] L. J. du Toit, "Cehphi'99: Dosimetry laboratory operations guide," Tech. Rep. LRAD-DL-05-R: Rev. A, EM Software & Systems, June 2000.

[16] *DASY3 Dosimetric Assessment System- Product Catalogue 1999.* Schmid & Partner Engineering AG, Zurich, Switzerland: http://www.speag.com.

[17] "Guidelines for limiting exposure to time-varying electric, magnetic, and electromagnetic fields (up to 300ghz)," tech. rep., ICNIRP (International Commission on Non-Ionizing Radiation Protection), Apr 1998.

[18] M. Okoniewski, *Totem User's Notes.* University of Victoria, Victoria, Canada, October 1999.

[19] F. J. C. Meyer and K. Palmer, "Numerical dosimetry research at EMSS: Development of generic cellphone models for use with the MoM and FDTD techniques in numerical SAR assessment.," Tech. Rep. 2000_P02_50, EM Software & Systems, Quantum Building, Technopark, Stellenbosch, South Africa, www.emss.co.za, June 2000.

[20] G. Lazzi and O. P. Gandhi, "On modeling and personal dosimetry of cellular telephone helical antennas with the FDTD code," *IEEE Trans. Antennas Propagat.*, vol. 46, pp. 525–529, Apr. 1998.

[21] J. Vaul and P. Excell, "Numerical Realisation of Realistic Articulated Hand Model for Mobile Telephone Dosimetry Studies," in *Proceedings of the Twenty Second Annual Meeting of the Bioelectromagnetic Society*, (Munich, Germany), p. 141, June 2000.

[22] "IEEE SCC34/sc-2, unapproved draft recommended practice document," Tech. Rep. IEEE SCC34/SC-2, IEEE, 2000.

[23] J. Wojcik and P. Cardinal, "New Advanced Methodology for Near Field Measurements for SAR and Antenna Development," in *1995 IEEE MTT-S Digest*, pp. 291–294, 1995.

[24] A. Tilley and H. Dreyfuss, *The Measure of Man and Woman: Human Factors in Design.* Watson-Guptill, 1993.

[25] "IEEE standard for safety levels with respect to human exposure to radio frequency electromagnetic field, 3 kHz to 300 GHz," Tech. Rep. IEEE C95.1-1991, IEEE, 1992.

[26] W. C. Chew, J.-M. Jin, C.-C. Lu, E. Michielssen, and J. M. Song, "Fast solution methods in electromagnetics," *IEEE Trans. Antennas Propagat.*, vol. 45, pp. 553–543, Mar. 1997.